Available online at www.sciencedirect.com
SCIENCE DIRECT®
Journal of Non-Crystalline Solids 351 (2005) 3121–3126
JOURNAL OF NON-CRYSTALLINE SOLIDS
www.elsevier.com/locate/jnoncrysol

A structural model of La_2O_3–Nb_2O_5–B_2O_3 glasses based upon infrared and luminescence spectroscopy and quantum chemical calculations

Wallace D. Fragoso [a], Celso de Mello Donegá [b], Ricardo L. Longo [a,*]

[a] Departamento de Química Fundamental, Universidade Federal de Pernambuco, 50740-540 Recife, PE, Brazil
[b] Debye Institute, Department of Physics and Chemistry of Condensed Matter, Utrecht University, P.O. Box 80000, 3508TA Utrecht, The Netherlands

Received 3 February 2005; received in revised form 23 July 2005

Abstract

Infrared spectra of $20La_2O_3$–xNb_2O_5–$(80-x)B_2O_3$, $24La_2O_3$–xNb_2O_5–$(76-x)B_2O_3$ and $28La_2O_3$–xNb_2O_5–$(72-x)B_2O_3$ glasses, with $x = 1$, 5, 10, 15 and 20, have been obtained. Also, the luminescence spectrum of the $28La_2O_3$–$10Nb_2O_5$–$62B_2O_3$ sample has been obtained. Density functional theory (DFT-B3LYP) calculations on clusters containing BO_3, BO_4, NbO_6, edge-sharing NbO_6–NbO_6, edge-sharing NbO_6–NbO_6 (niobyl), and corner-sharing NbO_6–NbO_6 groups have been used to aid the infrared spectra assignments. From these data it was possible to propose a structural model for the La_2O_3–Nb_2O_5–B_2O_3 glasses that is consistent with all the spectroscopic and theoretical results as well with previous luminescence study of similar samples. Briefly, this model consists of distorted NbO_6 octahedral groups replacing the BO_4 tetrahedral groups giving rise to non-bridging oxygen ions and distorted NbO_6 chains. These chains change from edge-sharing to corner-sharing distorted NbO_6 octahedra depending upon the La_2O_3 concentration. For La_2O_3 concentration larger than 28 mol% there seems to be a segregation of La(III) to another domain, restoring the structure observed for samples with La_2O_3 concentrations lower than 20 mol%.

PACS: 71.15.Mb; 78.30.−j; 78.55.−m; 81.05.Kf

1. Introduction

Glasses of composition xLa_2O_3–yM_2O_5–$(100-x-y)B_2O_3$ (M = Nb or Ta) have been developed for optical application and present interesting properties, such as, large chemical resistance and surface hardness, high refractive indices, excellent transparency in the visible–IR region and intense UV absorption. Glasses with a low M(V) contents show broad band luminescence upon UV excitation (blue for Ta and green for Nb). The increase in the M(V) concentration gives rise to energy migration among the MO_6^- groups [1].

The niobate luminescence has been extensively investigated in crystalline materials [2–6], and is strongly dependent upon the crystal structure. The most efficient luminescence occurs in niobyl groups [4], i.e., an Nb–O group with a short bond distance, ≈0.17 nm. Structurally isolated NbO_6 octahedra, such as in ordered perovskites and in $MgNb_2(P_2O_7)_3$ are not efficient luminescent centers [7], whereas isolated distorted niobate groups, such as in $LaNbO_4$, where the Nb(V) has a 4 + 2 coordination, provide very efficient centers [3]. Edge- or face-shared NbO_6 octahedral groups show efficient luminescence with a large Stokes shift, Δ_{ST}, i.e. the energy difference between the emission and excitation

* Corresponding author. Tel.: +55 81 2126 8440; fax: +55 81 2126 8442.
E-mail address: longo@ufpe.br (R.L. Longo).

0022-3093/$ - see front matter © 2005 Elsevier B.V. All rights reserved.
doi:10.1016/j.jnoncrysol.2005.07.031

maxima; while corner-sharing of NbO_6 groups leads to a shift of the optical absorption to lower energies, exciton delocalization, smaller Δ_{ST}; lower quenching temperatures, energy migration and consequently luminescence quenching [3].

The observation of niobate luminescence thus implies a considerable degree of short- and intermediate-range order in La_2O_3–Nb_2O_5–B_2O_3 glasses. In our previous work, we observed a relationship between the luminescence and the sample composition [8]. Crystalline niobate were used as model systems for extrinsic sub-networks in glasses structures. Even in samples at 20 mol% of La_2O_3 pairs of edge-sharing NbO_6 groups occur and the luminescence is typical for this structure. The increase of La_2O_3 concentrations at 25 mol% seems to disrupt these chains of niobate edge-sharing into corner-sharing off-center units. This leads to structural changes that are reflected into the luminescence properties [8].

In this work we reported the infrared spectroscopy study that agrees with our previous work hypothesis and expands the luminescence study for a sample with 28 mol% of La_2O_3.

2. Experimental and computational procedures

Glass samples of xLa_2O_3–yNb_2O_5–$(100 - x - y)B_2O_3$ ($x = 20$, 24, and 28, $y = 1$, 5, 10, 15 and 20) composition were prepared by melting 5 g batches at 1180 °C for 1 h, in Pt–5%Au crucibles, followed by quenching by pouring onto Pt plates at room temperature. The H_3BO_3 was used for obtaining the B_2O_3 and an excess of 12 wt% was added to compensate for evaporation losses. Considering that the melting temperature (1180 °C) is well below the fusion temperatures of La_2O_3 (2320 °C) and Nb_2O_5 (1512 °C), but larger than that of B_2O_3 (450 °C), it is safe to assume that B_2O_3 is the volatile species. Then, by mass differences it was shown for nine samples that the final compositions were within 0.5 mol% from the nominal ones, and for the same nominal compositions the differences were no larger than 0.04 mol%.

The samples were characterized by IR vibrational spectroscopy. The IR vibrational absorption spectra were measured on a Bruker IF566 spectrophotometer, using KBr pellet techniques.

Theoretical calculations were performed in order to aid the spectral assignments, and Fig. 1 presents the clusters used for these calculations. Structures I and II represent the BO_3 and BO_4 groups in a borate chain, respectively, whereas III, IV, V and VI contain the NbO_6 octahedra replacing the BO_4 group in the borate chain, the edge-sharing NbO_6 groups, the edge-sharing NbO_6 groups with only niobyl moiety, and the corner-sharing of NbO_6 groups, respectively. Geometry optimizations and vibrational frequencies calculations were performed with the Gaussian 98 program [9] with the hybrid-DFT B3LYP method [10]. The basis sets employed were LANL2DZ [11] with ECP for Nb, 6-31 + G [12] for O, and 6-31G [12] for B and H atoms. All calculations were performed without any symmetry constraints and the program default criteria were used for convergence and cutoffs.

The $28La_2O_3$–$10Nb_2O_5$–$62B_2O_3$ glass sample was studied with luminescence spectroscopy. The luminescence

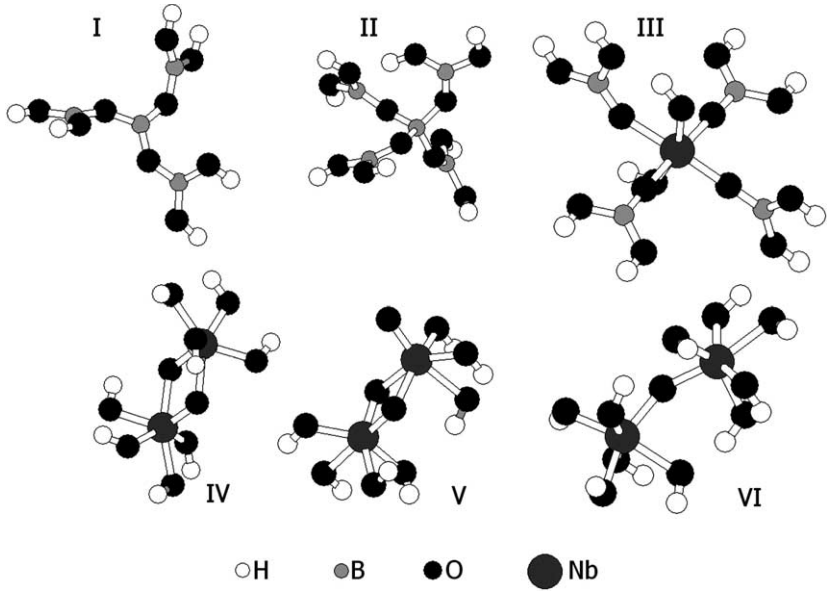

Fig. 1. Cluster models used in the calculation of the vibrational frequencies associated with BO_3, BO_4, NbO_6, edge-sharing NbO_6–NbO_6, edge-sharing NbO_6–NbO_6 (niobyl), and corner-sharing NbO_6–NbO_6 groups.

spectra were obtained by using a SPEX Fluorolog DM3000F spectrofluorometer with double-grating 0.22 m SPEX 1680 monochromators, and a 450 W Xe lamp as the excitation source. This setup is equipped with an Oxford LF205 liquid helium flow cryostat, allowing for measurements down to 4.2 K.

3. Results

Fig. 2 shows the vibrational spectra of $20La_2O_3$ glass series, and Figs. 3 and 4 present the vibrational spectra for 24 and $28La_2O_3$ glass series, respectively.

Table 1 presents the spectra assignment supported by the literature data [13,14] and the calculated vibrational frequencies.

The excitation and emission spectra of the $28La_2O_3$–$10Nb_2O_5$–$62B_2O_3$ glass sample are presented in Fig. 5.

In addition to these results obtained for the $28La_2O_3$–$10Nb_2O_5$–$62B_2O_3$ sample, Table 2 presents the luminescence results for other samples from our previous work [8] as well as for three other crystalline niobates.

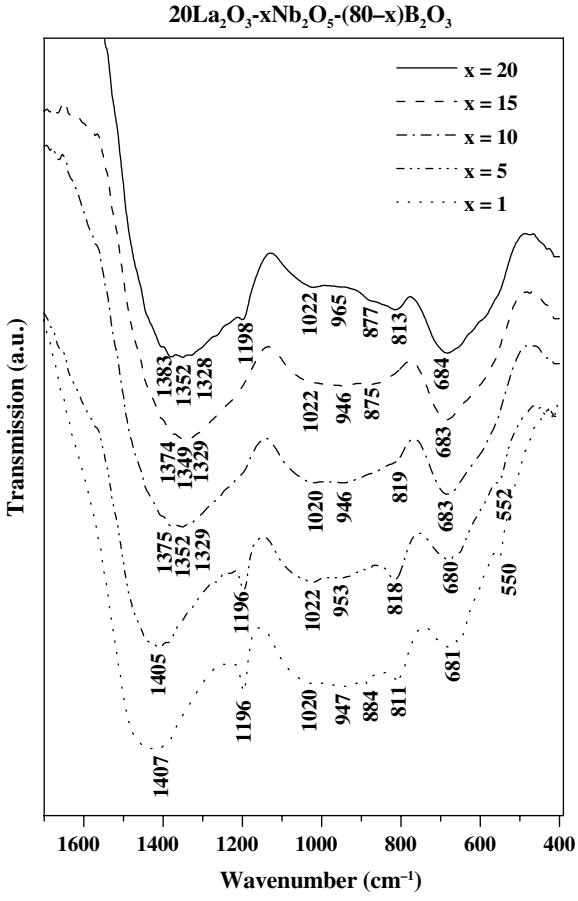

Fig. 2. Infrared spectra of $20La_2O_3$–xNb_2O_5–$(80 - x)B_2O_3$ glasses with $x = 1$, 5, 10, 15 and 20. The data have been plotted with a displacement in the y-axis (arbitrary units – a.u.) in order to improve visualization and comparison.

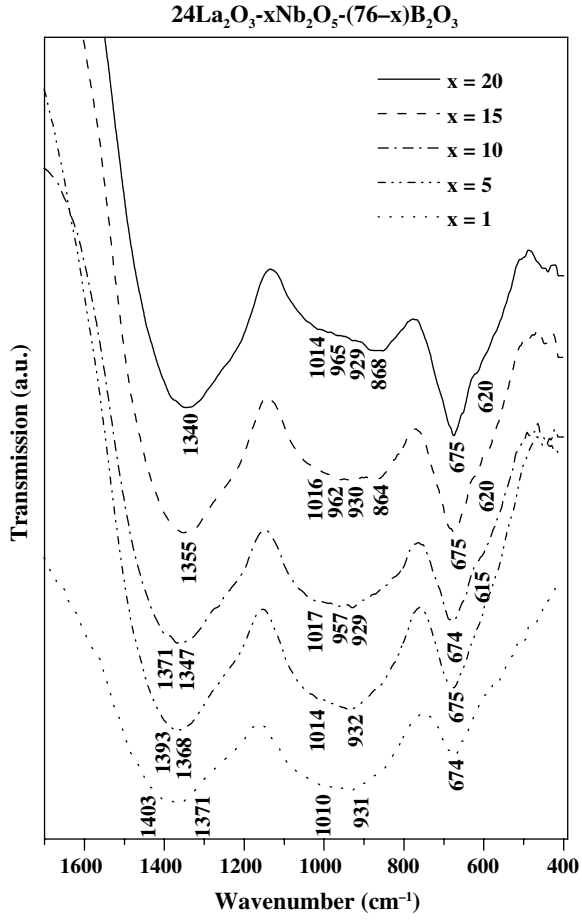

Fig. 3. Infrared spectra of $24La_2O_3$–xNb_2O_5–$(76 - x)B_2O_3$ glasses with $x = 1$, 5, 10, 15 and 20. The data have been plotted with a displacement in the y-axis (arbitrary units – a.u.) in order to improve visualization and comparison.

4. Discussion

All vibrational spectra present three broad bands in the 400–1700 cm^{-1} region according to Figs. 2–4. For all three series of samples, the intensities of the BO_4 group stretching vibrational frequencies (1020–1030 cm^{-1}) decrease and the intensities of the NbO_6 group characteristic vibrational frequencies (around 680 cm^{-1}) increase with the increase of Nb_2O_5 contents. These suggest that the distorted NbO_6 octahedra groups replace the BO_4 tetrahedral groups and give rise to non-bridging oxygen atoms.

Bands in the 550–560 cm^{-1} and 810–830 cm^{-1} regions, which are characteristics of edge-sharing niobate groups (Table 1), were observed in infrared spectra of the samples with 20 and 28 mol% of La_2O_3 (Figs. 2 and 4), but not in spectra with 24 mol% La_2O_3 (Fig. 3). We suppose that the increase of La_2O_3 concentration from 20 to 24 mol% disrupts the edge-sharing NbO_6 pairs, but that another increase to 28 mol% of La_2O_3 induces a phase segregation, which gives rise to a decrease of lanthanum concentration content around

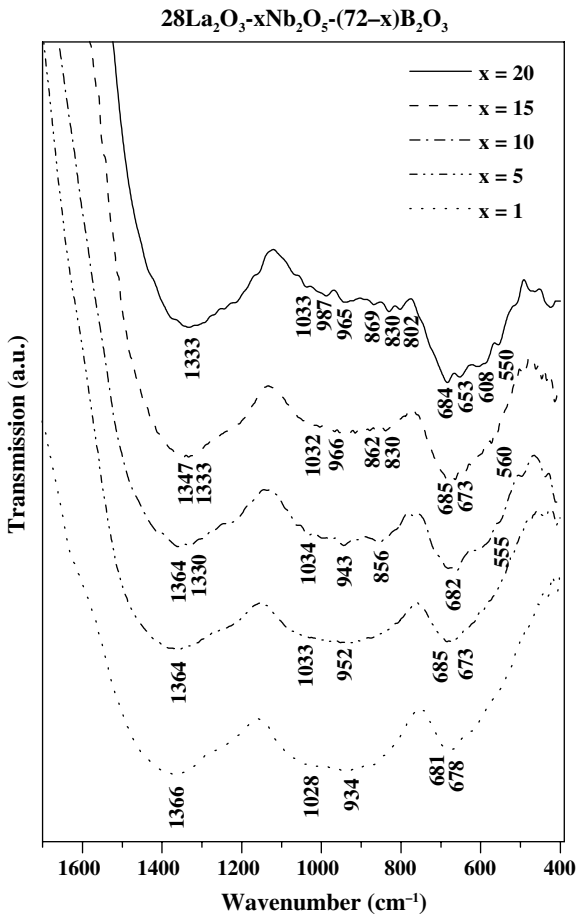

Fig. 4. Infrared spectra of $28La_2O_3$–xNb_2O_5–$(72 - x)B_2O_3$ glasses with $x = 1$, 5, 10, 15 and 20. The data have been plotted with a displacement in the y-axis (arbitrary units – a.u.) in order to improve visualization and comparison.

the niobates groups, thus increasing the formation of NbO_6 pair edge-sharing groups.

In order to ascertain this hypothesis we have studied the $28La_2O_3$–$10Nb_2O_5$–$62B_2O_3$ sample using luminescence spectroscopy. It is clear that if distorted octahedra

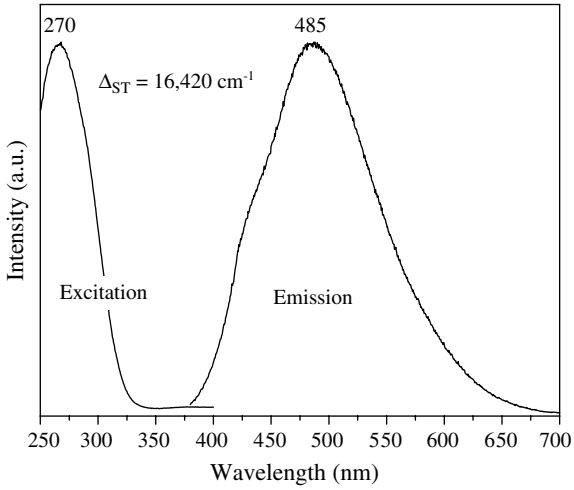

Fig. 5. Excitation and emission spectra at 4.2 K of the $28La_2O_3$–$10Nb_2O_5$–$62B_2O_3$ sample.

connected by the edges are present in the sample, then their characteristic luminescence would be observed.

The maximum excitation (λ_{exc}) and emission (λ_{em}) wavelengths were 270 and 485 nm, respectively, yielding a Stokes shift (Δ_{ST}) of 16420 cm^{-1}. These results are very close to those observed for crystalline $CaNb_2O_6$, namely $\lambda_{exc} = 260$ nm, $\lambda_{em} = 460$ nm and $\Delta_{ST} = 16000\ cm^{-1}$, which has a columbite structure characterized by edge-sharing distorted NbO_6 octahedra [15].

Based upon the present vibrational and luminescence spectroscopic results as well as our previous luminescence study [8] we are now able to propose a model for the structural changes with respect to the composition of the vitreous system La_2O_3–Nb_2O_5–B_2O_3. Even at concentrations as low as 1 mol% of Nb_2O_5 in 19–20 mol% of La_2O_3 it is possible to observe edge-sharing NbO_6 groups according to the observed vibrational frequencies in the 550 and 810–820 cm^{-1} region, which are also responsible for the observed luminescence in these

Table 1
Assignments of the vibrational bands (cm^{-1}) in the infrared spectra of borate and niobate groups

Assignment	Observed present work	Calculated present work	Literature [13,14]
B–O stretching in BO_3 groups (model **I**)	1330–1400	1320–1490	1220, 1330 and 1440
B–O stretching in BO_4 groups (model **II**)	960–1030	965, 1101 and 1138	900–1040
Nb–O stretching of the terminal oxygen atoms in the NbO_6 group connected to four BO_3 groups (model **III**)	670–685	682	–
Nb–O symmetric stretching of the edge-sharing oxygen atoms in the edge-sharing NbO_6 groups (model **IV**)	800–830	800	850
Nb–O asymmetric stretching of the terminal oxygen atoms in the edge-sharing NbO_6 groups (model **IV**)	550–560	530	500
Nb═O stretching of the niobyl in the edge-sharing NbO_6 groups (model **V**)	860–880	857	–
Nb–O–Nb symmetric stretching in the corner-sharing NbO_6 groups (model **VI**)	608–620	603	620 and 700

See Fig. 1 for the description of the models.

Table 2
Spectroscopic and structural properties at 4.2 K of crystalline and non-crystalline niobates

Structure	$\lambda_{em(max)}$	$\lambda_{exc(max)}$	Δ_{ST}
α-$LaNb_3O_9$ – double chains of distorted NbO_6 octahedra which share opposite corners along the chain and share edges across the chain, with Nb–O–Nb = 130°–155° [6]	535	310	14000
$CaNb_2O_6$ – columbite [15]	455	260	16500
α-$NbPO_5$ – single chains of corner-sharing distorted NbO_6 octahedra with Nb–O = 0.210 nm and Nb–O = 0.177 nm (niobyl), leading to approximately isolated niobyl groups [6]	490	260	18000
$19La_2O_3$–$1Nb_2O_5$–$80B_2O_3$	490	280	15300
$19La_2O_3$–$10Nb_2O_5$–$71B_2O_3$	510	290	14800
$19La_2O_3$–$20Nb_2O_5$–$61B_2O_3$	570	340	11800
$25La_2O_3$–$10Nb_2O_5$–$65B_2O_3$	510	265	18100
$28La_2O_3$–$10Nb_2O_5$–$62B_2O_3$	485	270	16420

Wavelengths (nm) at maximum of emission, $\lambda_{em(max)}$, and of excitation, $\lambda_{exc(max)}$, and Stokes shifts, Δ_{ST}, in cm^{-1}.

samples. As the Nb_2O_5 concentration increases from 1 up to 20 mol%, the niobate chains and the La(III) ions, intercalated within the borate chains, are organized similarly to the structure observed in α-$LaNb_3O_9$, namely, double chains of distorted NbO_6 octahedra which share opposite corners along the chain, and the double chains are interconnected by single chains of corner-sharing NbO_6 octahedra [6]. The luminescence of the La_2O_3–Nb_2O_5–B_2O_3 glass is then very similar to the luminescence of the crystalline α-$LaNb_3O_9$, yielding the best agreement when the glass composition is $19La_2O_3$–$10Nb_2O_5$–$71B_2O_3$ as observed in Table 2. The increase of the La_2O_3 concentration to 25 mol% causes the breakdown of the niobate chains so that the presence of edge-sharing NbO_6 groups is negligible, and the resulting structure is similar to that found in crystalline α-$NbPO_5$ [6]. This latter structure can be interpreted as corner-sharing distorted NbO_6 octahedra single chains, where the Nb(V) ion is not perfectly centered between the two oxygen ions, leading to approximately isolated niobyl groups. Corroborating this proposal is the fact that the bands associated with the edge-sharing niobate groups are not observed in the infrared spectra of the samples containing La_2O_3 24 mol%, whereas bands at 620 cm^{-1}, which are associated with corner-sharing NbO_6 groups, are quite intense. The further increase of the La_2O_3 concentration to 28 mol% causes the segregation of La_2O_3 into a distinct domain, where the excess of La(III) is probably segregated to this domain that should be structurally similar to the binary La_2O_3–B_2O_3 glass. As a result, the effective concentration of La(III) in the borate–niobate glass decreases allowing again the formation of edge-sharing niobate chains. This would also lead to an observed luminescence similar to that of crystalline α-$LaNb_3O_9$, which can be verified in Fig. 5 and Table 2. Consistent with these results are the infrared spectra for the glass samples with La_2O_3 at 28 mol% and Nb_2O_5, at concentration larger than 10 mol%, where the bands at 550 and 830 cm^{-1}, due to the edge-sharing NbO_6 groups, reappear as seen in Fig. 4. Also, for these samples the band at 680 cm^{-1} is broader compared to lower La_2O_3 concentrations, which might suggest the presence of a band at 640 cm^{-1} characteristic of binary La_2O_3–B_2O_3 glass [1].

5. Conclusions

The combination of infrared and luminescence spectroscopy with vibrational frequency calculations has provided a consistent structural model for the La_2O_3–Nb_2O_5–B_2O_3 glasses, where distorted NbO_6 octahedral groups replace the BO_4 tetrahedral groups giving rise to non-bridging oxygen ions. For concentrations of La_2O_3 lower than 20 mol% the results are consistent with the presence of edge-sharing distorted NbO_6 octahedra chains, even for Nb_2O_5 concentrations as low as 1 mol%. This structure is disrupted when the La_2O_3 concentration is increased up to 28 mol%, leading to corner-sharing distorted NbO_6 octahedra single chains with the presence of approximately isolated niobyl groups. Beyond 28 mol% of La_2O_3 there seems to be a segregation of La(III) to a binary La_2O_3–B_2O_3 glass domain, restoring the structure observed for samples with La_2O_3 concentrations lower than 20 mol%.

Acknowledgements

Partial financial support from the Brazilian agencies CNPq and PADCT is gratefully acknowledged. One of the authors (WDF) wishes to acknowledge CNPq and FACEPE for providing graduate scholarships. We are indebted to Professor A. Meijerink (Universiteit Utrecht, The Netherlands) for kindly allowing the use of his laboratory facilities.

References

[1] A.C.V. de Araújo, I.T. Weber, W.D. Fragoso, C.M. Donegá, J. Alloys Compd. 275–277 (1998) 738.

[2] G. Blasse, B.C. Grabmaier, Luminescent Materials, Springer, Berlin, 1994.

[3] G. Blasse, J. Solid State Chem. 72 (1988) 72.

[4] M.F. Hazenkamp, A.W.P.M. Strijbosch, G. Blasse, J. Solid State Chem. 97 (1992) 115.

[5] G. Blasse, G.J. Dirksen, Inorg. Chim. Acta 157 (1989) 141.

[6] H.C.G. Verhaar, H. Donker, G.J. Dirksen, M.J.J. Lammers, G. Blasse, C.C. Torardi, L.H. Brixner, J. Solid State Chem. 60 (1985) 20.

[7] J.W.M. Verwey, G. Blasse, Mater. Chem. Phys. 25 (1990) 91.

[8] W.D. Fragoso, C.M. Donegá, R.L. Longo, J. Lumin. 105 (2003) 97.

[9] M.J. Frisch, G.W. Trucks, H.B. Schlegel, G.E. Scuseria, M.A. Robb, J.R. Cheeseman, V.G. Zakrzewski, J.A. Montgomery Jr., R.E. Stratmann, J.C. Burant, S. Dapprich, J.M. Millam, A.D. Daniels, K.N. Kudin, M.C. Strain, O. Farkas, J. Tomasi, V. Barone, M. Cossi, R. Cammi, B. Mennucci, C. Pomelli, C. Adamo, S. Clifford, J. Ochterski, G.A. Petersson, P.Y. Ayala, Q. Cui, K. Morokuma, D.K. Malick, A.D. Rabuck, K. Raghavachari, J.B. Foresman, J. Cioslowski, J.V. Ortiz, B.B. Stefanov, G. Liu, A. Liashenko, P. Piskorz, I. Komaromi, R. Gomperts, R.L. Martin, D.J. Fox, T. Keith, M.A. Al-Laham, C.Y. Peng, A. Nanayakkara, C. Gonzalez, M. Challacombe, P.M.W. Gill, B. Johnson, W. Chen, M.W. Wong, J.L. Andres, C. Gonzalez, M. Head-Gordon, E.S. Replogle, J.A. Pople, Gaussian 98 (Revision A.6), Gaussian Inc., Pittsburgh PA, 1998.

[10] C.J. Cramer, Essentials of Computational Chemistry, John Wiley, New York, 2002.

[11] J.P. Hay, W.R. Wadt, J. Chem. Phys. 82 (1985) 299.

[12] W.J. Hehre, R. Ditchfield, J.A. Pople, J. Chem. Phys. 56 (1972) 2257;
P.C. Hariharan, J.A. Pople, Mol. Phys. 27 (1974) 209;
T. Clark, J. Chandrasekhar, G.W. Spitznagel, P.V.R. Schleyer, J. Comput. Chem. 4 (1983) 294.

[13] M. Tatsumisago, A. Hamada, T. Minami, M. Tanaka, J. Non-Cryst. Solids 56 (1983) 423.

[14] Z. Wang, B. Sui, S. Wang, H. Liu, J. Non-Cryst. Solids 80 (1986) 160.

[15] G. Blasse, M.G.J. van Leur, Mater. Res. Bull. 20 (1985) 1037.